Lawrence Berkeley National Laboratory

Title
A Cone Jet-Finding Algorithm for Heavy-Ion Collisions at LHC Energies

Permalink
https://escholarship.org/uc/item/4fd6j0st

Authors
Blyth, S.-L.
Horner, M.J.
Awes, T.
et al.

Publication Date
2008-05-09

A Cone Jet-Finding Algorithm for Heavy-Ion Collisions at LHC Energies

S-L Blyth[1,2]**, M J Horner**[1,2]**, T Awes**[3]**, T Cormier**[4]**, H Gray**[1,2]**, J L Klay**[5]**, S R Klein**[1]**, M van Leeuwen**[1]**, A Morsch**[6]**, G Odyniec**[1] **and A Pavlinov**[4]

[1] Lawrence Berkeley National Laboratory, Berkeley, California 94720, USA
[2] UCT-CERN Research Centre, University of Cape Town, Rondebosch 7700, South Africa
[3] Oak Ridge National Laboratory, Oak Ridge, Tennessee 37831, USA
[4] Wayne State University, Detroit, Michigan 48202, USA
[5] Lawrence Livermore National Laboratory, Livermore, California 94550, USA
[6] CERN, CH-1211 Geneva 23, Switzerland

Abstract. Standard jet finding techniques used in elementary particle collisions have not been successful in the high track density of heavy-ion collisions. This paper describes a modified cone-type jet finding algorithm developed for the complex environment of heavy-ion collisions. The primary modification to the algorithm is the evaluation and subtraction of the large background energy, arising from uncorrelated soft hadrons, in each collision. A detailed analysis of the background energy and its event-by-event fluctuations has been performed on simulated data, and a method developed to estimate the background energy inside the jet cone from the measured energy outside the cone on an event-by-event basis. The algorithm has been tested using Monte-Carlo simulations of Pb+Pb collisions at $\sqrt{s} = 5.5$ TeV for the ALICE detector at the LHC. The algorithm can reconstruct jets with a transverse energy of 50 GeV and above with an energy resolution of $\sim 30\%$.

1. Introduction

Jet-finding techniques, a well-established tool for $p + p$, $e^+ + e^-$ and $e + p$ collisions [1], are not directly applicable in heavy-ion (HI) collisions due to the overwhelming combinatorial backgrounds from high multiplicity underlying events. For central Pb+Pb collisions, nearly all 400 nucleons participate, leading to a high multiplicity of particles produced in simultaneous nucleon-nucleon collisions. In conventional jet-finding algorithms, this background energy will be swept up into the jet-cone, and strongly distort the reconstructed jet.

At RHIC (Relativistic Heavy-Ion Collider, $\sqrt{s_{NN}} = 200$ GeV), leading particle spectra and di-hadron correlations have been used to study jet production in heavy ion collisions. These measurements have revealed significant parton energy loss in the hot

and dense medium created in these collisions [2, 3, 4, 5]. Quantitative theoretical analysis of these results will greatly benefit from full jet reconstruction, which gives access to the parton energy before fragmentation, to disentangle various energy loss effects. At RHIC, however, full jet reconstruction is not possible due to limited kinematic reach (up to approx. 50 GeV for $p + p$ jets) and the large fluctuating background.

At the much higher LHC energies ($\sqrt{s_{NN}} = 5.5$ TeV for Pb+Pb), the cross-sections for hard processes are expected to be orders of magnitude larger than at RHIC while the background will increase by a smaller factor of about 4 (estimated from an extrapolation of charged particle rapidity density from SPS and RHIC). The growth of the jet cross-section from RHIC to LHC is illustrated in Fig. 1 which shows the differential cross-section for inclusive jets within a pseudorapidity range of $|\eta| < 1$ in $p + p$ collisions at RHIC and LHC energies as calculated by PYTHIA 6.2 [6] (left axis) and the expected annual yields in minimum bias Au+Au and Pb+Pb collisions (right axis). The Figure clearly shows that at 50 GeV, for example, the jet cross section is almost 5 orders of magnitude larger at LHC than at RHIC.

Studies of jet reconstruction on an event-by-event basis in large background Pb+Pb collisions at LHC energies have been pursued for some time by LHC heavy ion experiments [7, 8, 9]. In this paper, we present the first analysis based on simulations at mid-rapidity in the context of the ALICE experiment using charged particle tracking and electromagnetic calorimetry information for jet reconstruction.

Theoretical studies of partonic energy loss in a highly excited nuclear medium predict that jets with intermediate transverse energies ($50 \text{ GeV} \lesssim E_T \lesssim 100 \text{ GeV}$) may provide the best probe of the medium [10, 11, 12] since partons in this energy range are expected to suffer the greatest relative energy loss. Thus, the emphasis of the present analysis is on the reconstruction of jets in the transverse energy range from 50 to 100 GeV.

A cone-type jet-finding algorithm has been adapted from the UA1 experiment [13] and further developed to account for the heavy-ion background. The choice of various algorithm parameters and their influence on the jet energy resolution are discussed. The most challenging problem for jet-finding in heavy-ion experiments is the large, fluctuating background. Two methods for estimating the background were evaluated.

The presented simulations are based on the ALICE detector, using charged particle tracking for hadrons and an electromagnetic calorimeter for photon and electron detection. It has been shown previously that jets can be accurately reconstructed using this combination of detectors in $e^+ + e^-$ collisions at LEP (Large Electron Positron Collider) [14] and $p + \bar{p}$ collisions at the Tevatron [15]. This paper demonstrates that it can also be successful in the analysis of more complex heavy-ion collisions.
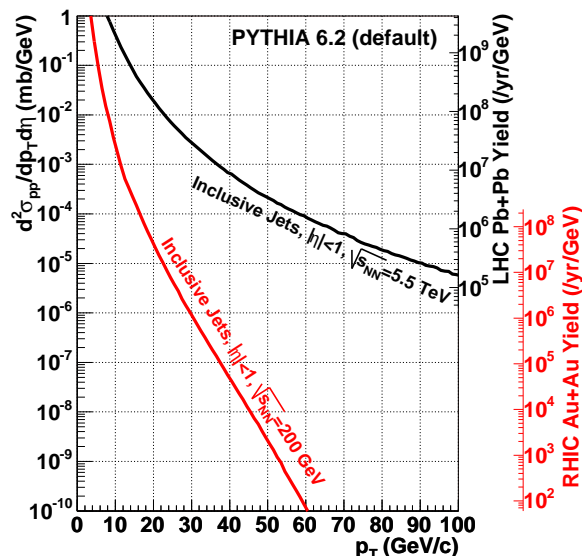
Figure 1. Differential cross-section for inclusive jets within $|\eta| < 1$ in $p + p$ collisions at RHIC and LHC from default PYTHIA 6.2 (left axis). The annual yields shown on the right axes are for minimum bias Pb+Pb (Au+Au) collisions assuming 10^6 s (10^7 s) running time and 0.5 mb^{-1} s^{-1} (5.0 mb^{-1} s^{-1}) luminosity at LHC (RHIC).

2. The Heavy-Ion Jet Algorithm (HIJA) and Simulations

2.1. Description of HIJA

This approach is based on a cone-type algorithm, developed by the UA1 collaboration [13], where the jet is defined as a group of particles in a cone of fixed radius in azimuth- (ϕ) and pseudorapidity- (η) space. The algorithm improvements evaluated by the Tevatron Run II Jet Physics Group [16], such as seedless cones, splitting/merging corrections and k_T algorithms [17], are not considered here but their feasibility could also be investigated for heavy-ion collisions.

The input to the algorithm is an energy grid in (η,ϕ) filled with a sum of transverse energy ($E_T^{Cell} = E \sin \theta_T$, where E is the total energy of the calorimeter cell and θ_T is the polar angle of the cell) measured by the electromagnetic calorimeter and charged track transverse momentum (p_T) information from the tracking system‡. The grid covers the same fiducial area as the calorimeter, and each grid cell corresponds in size and position to a calorimeter tower ($\eta \times \phi = 0.014 \times 0.014$ in ALICE [20]). In order to reduce the contributions from uncorrelated background particles, only charged hadrons with p_T above a threshold p_T^{cut} were used in the analysis. No cut was performed on calorimeter cell energy.

Neutral energy is measured only in the calorimeter while charged hadronic energy

‡ By adding p_T from charged particle tracking and E_T^{Cell} from the calorimeter in the grid cells, we neglect the contribution of the mass of charged hadrons to the jet energy. This effect is insignificant compared to the resolution effects under discussion in this paper.

is registered in both the tracking detectors and in the calorimeter. To correct for the double counting of hadronic energy, the estimated energy deposited by charged hadrons in the calorimeter is subtracted on a track-by-track basis using a parameterization of the average simulated energy deposition of charged pions in the calorimeter as a function of η and p_T, $\langle E_{HC}(\eta, p_T)\rangle$. For analysis of real data, the simulation of the hadronic response of the EMCal will have to be calibrated using test beams and data from peripheral collisions.

The algorithm consists of the following steps:

(i) Initialize the estimated background level per grid cell $\hat{E}_T^{BG}$ to be the average over all grid cells.

(ii) Sort cells in decreasing cell energy, E_T^i (where i is the index of the grid cell and runs from 1 to the total number of grid cells).

(iii) For at least 2 iterations, and until the change in $\hat{E}_T^{BG}$ between most recent successive iterations is smaller than a set threshold

   (a) Clear the jets list

   (b) Flag all grid cells as outside a jet

   (c) Execute the jet-finding loop for each grid cell, starting with the largest:

      1. If $E_T^i - \hat{E}_T^{BG} > E_T^{seed}$, where E_T^{seed} is a chosen threshold cell energy, and the grid cell is flagged as not in a jet, treat it as a jet seed candidate:

        (A) Set jet centroid (η^C, ϕ^C) to the co-ordinates of the jet seed cell η_i, ϕ_i.

        (B) Using all grid cells within $\sqrt{(\eta^i - \eta^C)^2 + (\phi^i - \phi^C)^2} < R$ of the initial centroid, calculate the new energy-weighted $(E_T^i - \hat{E}_T^{BG})$ centroid. Set the new energy-weighted centroid to be the new initial centroid. Repeat centroid calculation iterations until the centroid does not shift by more than one grid cell in subsequent iterations.

        (C) Store centroid as jet candidate and flag all grid cells within R of centroid as inside a jet.

   (d) Recalculate the estimated background energy $\hat{E}_T^{BG}$ using the calculation described in Section 3.1 (using all grid cells outside the cone).

   (e) For each jet candidate, calculate the energy by summing the energies of the grid cells in the cone and subtracting the background. If the jet energy is greater than E_T^{cone}, the minimum allowed cone energy, a jet is found.

The main algorithm parameters and their purposes are listed in Table 1.

Parameter	Description	Value	
E_T^{seed}	Minimum jet seed energy (after background subtraction)	4.6	GeV
R	Radius of jet cone	0.3	
E_T^{cone}	Minimum jet cone energy (after background subtraction)	14.0	GeV
p_T^{cut}	Minimum track p_T	2.0	GeV/c

Table 1. Main parameters used in HIJA.

2.2. Description of Detector and Simulated Events

Simulations of Pb+Pb collisions were performed for the ALICE experimental set-up using the ALICE software framework, AliRoot [18].

The ALICE tracking detector response was approximated using a gaussian smearing (with $\sigma = 1\%$) of the track momentum p and a conservative tracking efficiency of 90% (the presently anticipated ALICE tracking efficiency is 98% [19]). The ALICE electromagnetic calorimeter§, a sampling calorimeter with a projective geometry in η, composed of 25 layers of 5mm × 5mm Pb-scintillator corresponding to 21 radiation lengths, was simulated using full GEANT 3.21 shower evolution. The intrinsic energy resolution for photons with energies from 25 to 200 GeV for this device was estimated from simulation to be $\sigma(E)/E \sim 15\%/\sqrt{E}$ [20]. The calorimeter was simulated with a fiducial acceptance of $|\eta| < 0.7, \pi/3 < \phi < \pi$ and a granularity of 13 824 cells $(96(\eta) \times 144(\phi))$.

A sample of heavy-ion events with high energy jets of known energies was constructed by combining the output from two Monte Carlo event generators. Jet events were generated using PYTHIA 6.2 [6] and these were combined with high-multiplicity Pb+Pb 'background' events generated by HIJING 1.36 [21]. To define the input jet energy scale in PYTHIA events, the PYCELL algorithm‖ was used.

Calibration samples of $E_T = 50$ and 100 GeV (±5 GeV) jets were generated using PYTHIA. The jet directions were restricted in pseudorapidity ($|\eta| < 0.3$) and in azimuthal angle (more than 15 degrees, 0.26 radians from the edge of the calorimeter) to reduce the effect of the acceptance edges on the energy reconstruction. The jet energy and direction selection criteria were based on the output from PYCELL. The background event sample was composed of central HIJING events (impact parameter¶ $b < 5$ fm for the 10% most central collisions). The HIJING parameters were tuned for LHC energies according to [22]. The charged particle rapidity density in these events is approximately 4000 at mid-rapidity. This is likely to be an overestimate of the uncorrelated background [23] at LHC.

3. Background Energy Estimation and Choice of Algorithm Parameters

Parton energy loss effects are expected to be most visible in jets with $E_T \lesssim 100$ GeV [10, 11, 12]. The algorithm parameters were chosen to optimize the energy resolution for jets with $E_T = 50$ GeV since in the range of interest ($50 \lesssim E_T \lesssim 100$ GeV) this is the most challenging case to reconstruct.

§ The final design is still under evaluation. However, the changes under consideration are unlikely to affect jet reconstruction.
‖ PYCELL is the internal PYTHIA cone algorithm with $R = 1$ which uses all simulated particles to reconstruct jets.
¶ In heavy-ion collisions, the impact parameter b is defined as the distance of closest approach between the centres of the colliding nuclei. The most central collisions have the smallest impact parameter.

3.1. Background energy estimation

In this section simulated $p + p$ and Pb+Pb events are used to compare reconstructed jet energies to the background level and optimise the background estimation.

The left panel of Fig. 2 shows a comparison of the reconstructed jet energy and RMS for 50 GeV (triangles) and 100 GeV jets (squares) in $p + p$ events and the total background energy (circles) from uncorrelated particle production in Pb+Pb events, as a function of cone radius R. All points include a p_T-cut of 2 GeV/c on charged tracks which rejects most of the background from charged particles (98% on average in central HIJING events). While the measured jet energy only increases for small cone radii, up to $R \sim 0.3$, the background energy increases quadratically with R, exceeding 100 GeV at $R \sim 0.4$. However, since the background level can be subtracted on average, it is not so much the overall background level, but rather the event-by-event fluctuations in the background that are of interest.
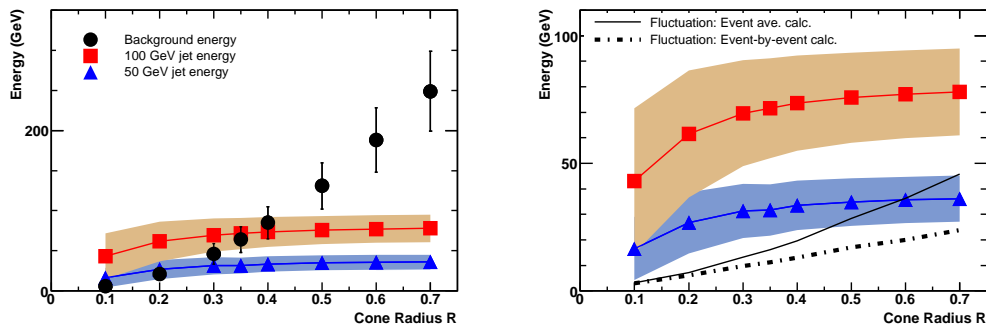
Figure 2. Left panel: Mean and RMS of background energy from central Pb+Pb background events (circles) compared to jet energy (simulated) from $p + p$ events for 50 GeV (triangles) and 100 GeV (squares) jets within jet cones of varying size R. The shaded bands around the jet energy symbols and vertical bars on the background symbols represent the RMS values of the distributions. Right panel: Jet energy within the cone for varying cone sizes (triangles: 50 GeV jets, squares: 100 GeV jets) compared to the central Pb+Pb background energy RMS in the cone calculated using two methods (solid line: event-averaged method, dot-dashed line: event-by-event method). The bands represent the RMS of the jet energy distributions.

In the right panel of Fig. 2, the reconstructed jet energy for 50 GeV (triangle markers) and 100 GeV jets (square markers) is compared to the fluctuations of the uncorrelated background. The solid line shows the RMS of the background energy (vertical bars in left panel) from central Pb+Pb events.

One of the sources of background energy fluctuations is fluctuations in the impact parameter of the collisions. The contribution of impact parameter fluctuations to the final jet energy resolution can be suppressed by estimating the energy from uncorrelated particles on an event-by-event basis from the total energy deposited outside the jet cone. For maximum statistical precision, we used the average total E_T per cell from the entire area of the jet-finding grid outside the cone, without applying the p_T-cut
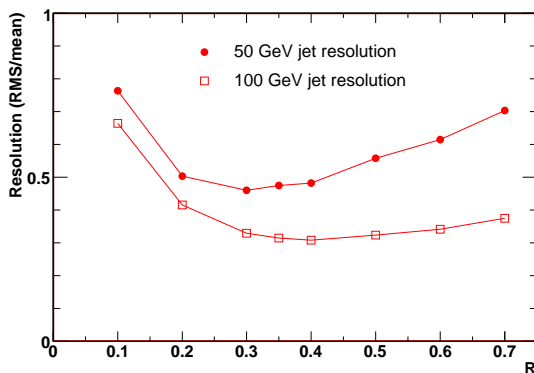
Figure 3. Energy resolution calculated as described in the text for 50 GeV jets (circles) and 100 GeV jets (squares) as a function of the cone radius R.

on charged tracks, $\langle E_T^{cell,nocut} \rangle$, as the basis for the background energy estimate. The actual background energy inside the jet-cone, with cuts, is then estimated by multiplying $\langle E_T^{cell,nocut} \rangle$ by an average correction factor F to account for the effect of the p_T-cut. The factor F is calculated as the ratio of the average cell-energy in the jet-finding grid with cuts to the case without cuts, averaged over the entire sample of background events. When the analysis is applied to experimental data, F can be calculated from events without detectable jets.

The resulting fluctuations of the true background energy (from HIJING Pb+Pb events) around the estimated background energy using this procedure is indicated by the dashed line in the right panel of Fig. 2. The event-by-event estimate of the background reduces the effect of fluctuations by about a factor 2. As a result, larger cone radii can be used for jet-finding. The remaining fluctuations are dominated by fluctuations due to the finite statistical precision of the background estimate.

3.2. Choice of parameters: cone radius

To determine the optimal cone radius for jet energy measurements in the presence of heavy ion backgrounds, we use a simple estimate of the relative energy resolution $\sigma(E_T)/E_T$ as a function of cone radius R. The relative energy resolution is estimated as the quadratic sum of the jet energy resolution $\sigma(E_T^{jet})$ in $p + p$ collisions and the fluctuations of the background energy, E_T^{BG}, around the estimated background $\hat{E}_T^{BG}$:

$$\sigma(E_T)/E_T \lesssim \frac{1}{E_T} \sqrt{\sigma(E_T^{jet})^2 + \sigma(E_T^{BG} - \hat{E}_T^{BG})^2} \tag{1}$$

Figure 3 shows the dependence of the relative jet energy resolution on the cone radius R. The relative jet energy resolution $\sigma(E_T)/E_T$ was calculated using Eq. 1. The RMS of the jet energy in $p + p$ collisions as shown in Fig. 2 was used for $\sigma(E_T^{jet})$ and the RMS of the background fluctuations (dash-dotted line in Fig. 2) was used for $\sigma(E_T^{BG} - \hat{E}_T^{BG})$. For small values of R, the jet energy resolution improves with increasing R because in-and-out-of-cone fluctuations dominate (first term in Eq. 1). At larger R,

the background fluctuations dominate and the resolution degrades with increasing R. For this study we chose the cone radius ($R = 0.3$) which resulted in the best energy resolution for 50 GeV jets. This result demonstrates that for optimum jet resolution in heavy-ion collisions, the jet cone must be restricted in size, with an optimum size that decreases with decreasing jet energy. Such restrictions will be necessary to enable jet reconstruction to the lowest jet energies in central Pb+Pb collisions. The biases introduced on the jet selection by such restrictions will require extensive systematic study, including comparisons with p+p reference data and theoretical calculations.

3.3. Choice of parameters: seed energy and minimum jet energy

Finding the optimal values for the jet seed energy, E_T^{seed}, and minimum accepted cone energy, E_T^{cone}, involves a trade-off between jet-finding efficiency and sample purity. To investigate this trade-off, we use HIJA on 'parameterized Pb+Pb' events. These events contain only pions and kaons sampled from the p_T and pseudorapidity distributions of the particles in HIJING events and are therefore free of jets by construction. The parameterized Pb+Pb events had a fixed charged particle rapidity density of $dN_{ch}/dy = 4\,000$ at mid-rapidity.

The values for $E_T^{seed} = 4.6$ GeV and $E_T^{cone} = 14.0$ GeV were selected because they resulted in (1) a high efficiency for finding 50 GeV embedded jets in Pb+Pb events and (2) a low number of 'fake' jets reconstructed in simulated Pb+Pb events. The efficiency and fake rates for jet-finding with these parameters are shown in Table 2. The efficiencies are 70% for 50 GeV jets and 97% for 100 GeV jets embedded in central HIJING background events. The fake rate is 3% in parameterized HIJING. The algorithm also finds jets in about 13% of the HIJING events. This is likely dominated by low energy 'real' jets in the events (the HIJING generator does not tag the generated jets, so it is not possible to verify this in more detail).

| | Param. | Pure | 50 GeV jets | 100 GeV jets |
	HIJING	HIJING	+ HIJING	+ HIJING
Accepted	3%	13%	70%	97%

Table 2. Percentage of the event sample accepted by the algorithm as containing a jet using $E_T^{seed} = 4.6$ GeV and $E_T^{cone} = 14.0$ GeV.

4. Results

This section summarizes the HIJA algorithm results for jet efficiency, energy and direction resolution in simulated Pb+Pb collisions. The values of the algorithm parameters used in this study are summarised in the right-most column of Table 1.

The jet-finding efficiencies in simulated Pb+Pb collisions with these cuts are given in Table 2 and found to be greater than 70% for jets of 50 GeV and above.

4.1. Direction resolution

The accuracy with which HIJA reconstructs jet directions is shown in Fig. 4 by the RMS values of the difference between the reconstructed and input jet directions (calculated by PYCELL), $\Delta\eta$ (triangles) and $\Delta\phi$ (circles) for Pb+Pb (solid) and $p + p$ (open). In $p + p$ and Pb+Pb events, the direction resolution is similar in η and ϕ, as one would expect from the fragmentation process, which is (approximately) symmetric in η and ϕ at mid-rapidity. At all energies, the uncorrelated background in Pb+Pb events leads to a slightly worse direction resolution than in $p + p$ events. The difference between the resolutions in $p + p$ and Pb+Pb events decreases with energy due to the increasing signal to background ratio.

In $p + p$ events, the jet direction resolution becomes slightly worse at higher jet energies due to the small cone radius of $R = 0.3$, which occasionally leads to two reconstructed jets instead of one. This "splitting" effect results in a small fraction of large $\Delta\eta$ and $\Delta\phi$ values, increasing with jet energy. The effect is also present in Pb+Pb, but it is offset by the background fluctuations. Possible corrections for this effect are discussed in [16].
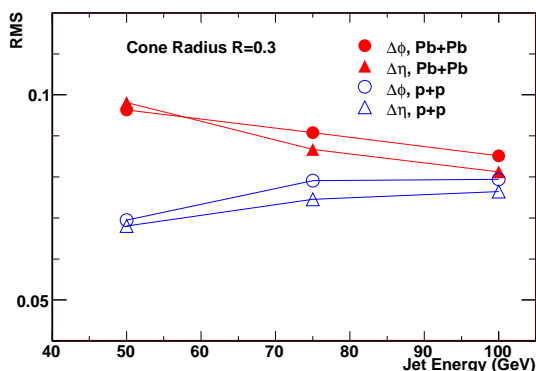
Figure 4. RMS of jet $\Delta\eta$ and $\Delta\phi$ distributions for the Pb+Pb (solid symbols) and $p + p$ (open symbols) cases as a function of jet energy for $R = 0.3$.

4.2. Jet energy resolution

Figure 5 shows the energy distributions of reconstructed jets that have been embedded in simulated central Pb+Pb events, using the optimized algorithm parameters (Table 1). Distributions are shown for both the raw reconstructed jet energy E_T^{Reco} and the corrected jet energy E_T^{Corr}. The reconstructed jet energies E_T^{Reco} were corrected for losses due to the small cone radius, the track p_T cut, and missing energy from unmeasured particles by multiplication with an average correction factor $C = 1/0.6731$, calculated from the (PYTHIA) simulations[+]. The factor is averaged with cross-sectional weight,

[+] When data become available, this procedure should be verified using p+p data and, if possible, γ-jet events.

and therefore reproduces the actual jet energy better at low energy. The solid lines represent Gaussian fits to the corrected jet energy distributions and are used to extract the width σ of the distributions.

The mean values and σ of the corrected energy distributions are given in Table 3. The mean values are within 4% of the input jet energies for all three samples.
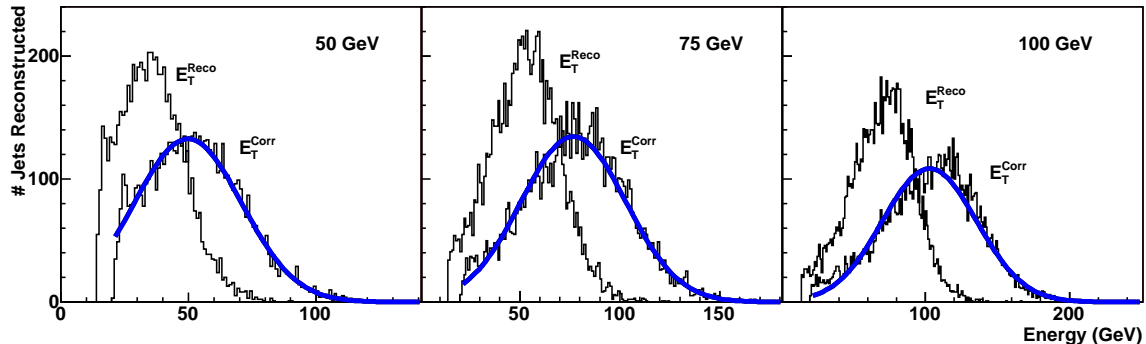
Figure 5. Reconstructed (E_T^{Reco}) and corrected (E_T^{Corr}) jet energy distributions for 50 GeV, 75 GeV and 100 GeV jets embedded in central Pb+Pb HIJING events.

	50 GeV jets + HIJING	**75 GeV jets** + HIJING	**100 GeV jets** + HIJING
$\langle E_T^{Reco}\rangle \pm \sigma$ **(GeV)**	34 ± 14	52 ± 18	70 ± 22
$\langle E_T^{Corr}\rangle \pm \sigma$ **(GeV)**	50 ± 21	77 ± 26	103 ± 33

Table 3. Mean value and standard deviation (σ) (taken from the Gaussian fits) of the reconstructed jet energy distributions (embedded in central Pb+Pb HIJING events) for various input jet energies before and after correction for losses due to the small cone radius, the track p_T cut, and missing energy from unmeasured particles.

## 5. Comparison to $p + p$ collision baseline

To further separate the effects of the various algorithm cuts and the effect of background fluctuations, we have studied the effects of the algorithm cuts on $p + p$ simulations. For this purpose a cross-section weighted spectrum of PYTHIA jets with PYCELL transverse energies between 20 and 180 GeV was generated. The influence of the HIJA cuts was examined by performing jet-finding directly on the PYTHIA particle lists without detector response simulation. HIJA results for jet-finding using all particle information and cone radius $R = 1.0$, agree with the reference spectrum from PYCELL.

Figure 6 shows the resolutions using HIJA on the PYTHIA spectrum, as a function of energy, for two choices of R and p_T-cut. To determine the energy resolution as a function of jet energy, jets were selected from the generated spectrum in a narrow (± 5 GeV) energy range around the values indicated by the data points. The spread of the reconstructed energies due to the width of the selected interval was taken out
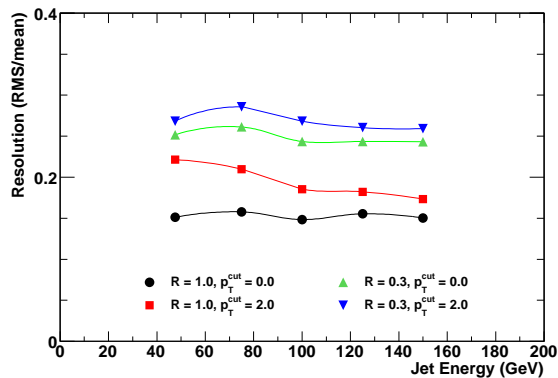
Figure 6. Energy resolution as a function of input jet energy for various HIJA cut combinations on p+p PYTHIA events without detector simulation.

by subtracting the nominal trend of reconstructed energy as a function of input energy. The RMS of the reconstructed energy distributions is used to characterise the resolution, because some of the distributions are not gaussian in shape. It should also be noted that the E_T^{cone} cut rejects a significant fraction of reconstructed jets at 50 GeV (see Table 2). The RMS is calculated with this cut imposed. The resolution for the ideal case (no cuts), but excluding undetectable particles (ν, K_L and neutrons) is approximately 15%, independent of energy (solid circle symbols). Application of the cuts on charged particle p_T and reducing the cone radius to $R = 0.3$ leads to additional loss of resolution as shown by the square and triangle markers. The final heavy-ion optimized parameters, as given in Table 1, leads to a resolution of 25–30% for jets with 50 GeV $< E_T <$ 160 GeV (down-pointing triangle markers). This is the intrinsic limit of the jet resolution in $p+p$ using HIJA with cuts optimized for central Pb+Pb.
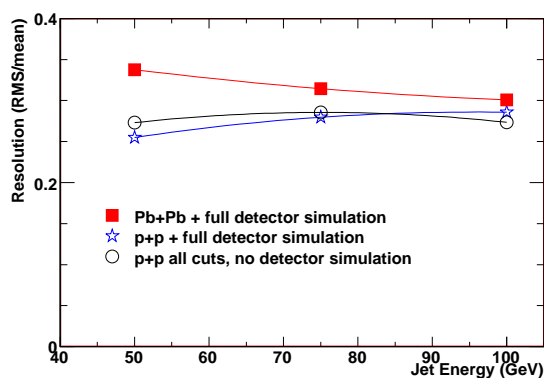
Figure 7. Reconstructed jet resolution (RMS/mean) as a function of energy for the Pb+Pb case including detector effects (solid squares), $p + p$ case including detector effects (open stars) and $p + p$ case without detector effects (open circles).

Figure 7 illustrates the effect of detector energy resolution and background fluctuations in Pb+Pb events by comparing the 'ideal' jet energy resolution in $p + p$

(PYTHIA without detector simulation and excluding v, K_L^0 and neutrons, open circles) with the actual jet energy resolution obtained with HIJA including all detector effects for the $p+p$ (open stars) case and detector and high multiplicity background effects for the Pb+Pb (solid squares) case.

The combination of detector effects (open stars) and including possible interactions of K_L^0 and neutrons in the detector material do not produce significant differences compared to the pure PYTHIA case (open circles). The small loss in jet energy resolution in $p+p$ from 50 to 100 GeV is an artifact of the E_T^{cone} cut. In Pb+Pb the contribution from the fluctuating background leads to an additional spread of the reconstructed jet energy, varying from $\sim$8% for 50 GeV jets, down to $<$2% for 100 GeV jets.

6. Summary and Conclusions

A UA1-based cone algorithm has been adapted to reconstruct jets in Pb+Pb collisions at $\sqrt{s_{NN}} = 5.5$ TeV at the LHC. A technique to estimate and subtract the background in heavy-ion collisions on an event-by-event basis has been developed. The contributions to the jet energy resolution from in-and-out-of-cone fluctuations, undetectable particles and the various algorithm cuts were studied. It has been shown that using this algorithm with the simulated ALICE detectors, jets of 50 GeV and higher transverse energies can be reconstructed on an event-by-event basis. The $p+p$ resolutions are significantly affected by the choice of parameters required to suppress the background in heavy-ion collisions. The final resolutions obtained with the selected algorithm parameters is $\sim$34%($\sim$26%) for 50 GeV jets and $\sim$30%($\sim$28%) for 100 GeV jets in Pb+Pb($p+p$) collisions. The main contribution to the degradation of the jet energy resolution in Pb+Pb compared to $p+p$ is due to the fluctuating underlying event. This background is intrinsic to heavy-ion collisions and will be present in all experiments at the LHC. Using these techniques will allow access to differential studies of parton energy loss and the properties of the dense nuclear medium created at the LHC.

Acknowledgements

[1] Ellis S D and Soper D E, *Phys. Rev.* D **48** (1993) 3160
[2] Gyulassy M and Plumer M, *Phys. Lett.* B **243** (1990) 432
[3] Wang X-N, *Phys. Rep.* **280** (1997) 287
[4] Wang X-N and Gyulassy M, *Phys. Rev. Lett.* **68** (1992) 1480
[5] Wang X-N, Huang Z and Sarcevic I, *Phys. Rev. Lett.* **77** (1996) 231
[6] Sjostrand T *et al*, *Computer Physics Commun.* **135** (2001) 238
[7] A. Accardi *et al*, *J. Phys.* G **30** (2004) S1155

[8] G. Baur *et al*, *Eur. Phys. J.* C **32** (2004) s69

[9] S.-L. Blyth *et al* (ALICE-USA collaboration), *Eur. Phys. J.* C **32** (2004) S1155

[10] Salgado C A and Wiedemann U A, *Phys. Rev.* D **68** (2003) 014008

[11] Vitev I and Gyulassy M, *Phys. Rev. Lett.* **89** (2002) 252301

[12] Wang Q and Wang X-N, *Phys. Rev.* C **71** (2005) 014903

[13] Arnison G A, *et al*, *Phys. Lett.* B **132** (1983) 214

[14] Buskulic D, *et al*, *Nucl. Instr. and Meth. in Physc. Res.* A **360** (1995) 481

[15] Bocci A, PhD Thesis (CDF), University of Pisa (1998) *unpublished*

[16] Blazey G C *et al*, hep-ex/0005012 v2

[17] Catani A, Dokshitzer Y L, Seymour M H and Webber B R, *Nucl. Phys.* B **406**, 187 (1993)

[18] http://aliceinfo.cern.ch/Offline/AliRoot/Manual.html

[19] *ALICE TDR of the Time Projection Chamber* , CERN/LHCC 2000-001

[20] ALICE-USA Collaboration, Proposal for an Electromagnetic Calorimeter for ALICE at the LHC (2003)

[21] Wang X-N and Gyulassy M, *Phys. Rev.* D **44** (1991) 35017

[22] Wang X-N, *Private Communication*: IHPR2(50) = 1, HIPR1(14) = 1.36, HIPR1(11) = 3.7

[23] *ALICE Physics Performance Report* , CERN/LHCC 2003-049 (November 2003)